

AperTO - Archivio Istituzionale Open Access dell'Università di Torino

Linking oral bioaccessibility and solid phase distribution of potentially toxic elements in extractive waste and soil from an abandoned mine site: Case study in Campello Monti, NW Italy

This is the author's manuscript

Original Citation:

Availability:

This version is available <http://hdl.handle.net/2318/1684764> since 2021-12-28T13:56:08Z

Published version:

DOI:10.1016/j.scitotenv.2018.10.115

Terms of use:

Open Access

Anyone can freely access the full text of works made available as "Open Access". Works made available under a Creative Commons license can be used according to the terms and conditions of said license. Use of all other works requires consent of the right holder (author or publisher) if not exempted from copyright protection by the applicable law.

(Article begins on next page)

1 **Linking oral bioaccessibility and solid phase distribution of potentially toxic elements in**
2 **extractive waste and soil from an abandoned mine site: Case study in Campello Monti, NW**
3 **Italy**

4 Neha Mehta^{1*}, Tatiana Cocerva², Sabrina Cipullo³, Elio Padoan⁴, Giovanna Antonella Dino¹,
5 Franco Ajmone Marsan⁴, Siobhan Cox², Frederic Coulon³, Domenico Antonio De Luca¹

6
7 ¹Department of Earth Sciences, University of Torino, Italy

8 ²School of Natural and Built Environment, Queen's University Belfast, UK

9 ³School of Water, Energy and Environment, Cranfield University, UK

10 ⁴ Department of Agricultural, Forest and Food Sciences, University of Torino, Italy

11 * Corresponding author, Email address : neha.mehta@unito.it

12

13 **Highlights**

- 14 • Extractive waste and soil at abandoned mines pose a risk to human health.
- 15 • Cr, Cu and Ni were present in high total concentrations at Campello Monti site.
- 16 • Potentially toxic elements were associated with clay and Fe oxide fractions.
- 17 • Mean BAF <11% for both Cr and Ni. Non-mobile form in Fe oxide fraction.
- 18 • PTE were found to be embedded in mineral grains of soil.

19

20 **Abstract**

21 Mining activities have led to the introduction of high levels of potentially toxic elements (PTE) in
22 soils. This has attracted governmental and public attention due to their non-biodegradable nature
23 and hazards posed to human health and the environment. However, total concentrations of PTE are
24 poor indicators of actual hazard to human health and can lead to overestimation of risk. In this
25 study, oral bioaccessibility, the fraction available for absorption via oral ingestion, was used to
26 refine human health risk assessment at an abandoned mine site from Campello Monti, north-west

27 Italy. The solid phase distribution was performed to characterise the distribution and the behaviour
28 of PTE within the extractive waste streams and impacted soil nearby. Mineralogical information
29 was obtained from micro-XRF and SEM analysis used to identify elemental distribution maps. The
30 results showed that the total concentrations of PTE were high, up to 7400 mg/kg for Ni due to the
31 presence of parent material, however, only 11% was bioaccessible. Detailed analysis of the
32 bioaccessible fraction (BAF) showed that As, Cu and Ni varied from 7 to 22%, 14 to 47%, 5 to
33 21%, respectively. The variation can be attributed to the difference in pH, organic matter content
34 and mineralogical composition of the samples. Non-specific sequential extraction also showed that
35 the non-mobile forms of PTE were associated with the clay and Fe oxide components of the
36 environmental matrices. The present study demonstrates how bioaccessibility, solid phase
37 distribution and mineralogical analysis can help decision making and inform the risk assessment of
38 abandoned mine sites.

39 Keywords: abandoned mine site, oral bioaccessibility, potentially toxic elements (PTE), risk
40 assessment, solid phase distribution.

41

42 **1. Introduction**

43 Since the onset of the industrial revolution, mining and smelting activities have been at the forefront
44 of economic development of many countries. Mining activities generate employment, while also
45 producing a wide variety of minerals that can have countless uses in various contexts (Ono et al.,
46 2016 ; Dino et al., 2018). Yet, mining and dressing activities have resulted in the generation of large
47 quantities of waste and degraded soils. After the closure of mines, these waste dumps were
48 abandoned. Further to this, the degraded soils, waste dumps and tailings are often geotechnically
49 unstable and sources of contamination by PTE (Gál et al., 2007). As PTE tend to persist in the
50 environment, these extractive waste dumps and soils often become a matter of concern for human
51 health (Lim et al., 2009).

52 There is growing awareness and concern about the harmful effects of elevated
53 concentrations of toxic elements on human health (Golia et al., 2008). However, there is growing
54 evidence that an elevated concentration of elements may not be indicative of the actual damaging
55 effects. Consequently, it has been proposed that bioavailable concentrations should be used to
56 inform human health risk assessment (HHRA). In the context of the present research, the
57 bioavailable concentration is the concentration of the contaminants reaching to the systemic
58 circulation (bloodstream) and thus is able to reach all target organ sites (Oomen, 2000). However,
59 measuring bioavailability in vivo is a difficult and lengthy procedure (Maddaloni et al., 1998).
60 Therefore, a number of in.vitro bioaccessibility methods have been developed to measure the oral
61 bioaccessibility of a contaminant (Cox et al., 2013). The oral bioaccessible fraction is defined as the
62 fraction that, after ingestion, may be mobilized into the gut fluids (chyme). Bioaccessible
63 concentration is greater than or equal to the bioavailable concentration and can be used as a
64 conservative measure to the bioavailability for HHRA (Paustenbach, 2000).

65 The in vitro bioaccessibility methods measure the oral bioaccessibility of PTE by mimicking
66 the stomach and intestine biochemical conditions. Some of the commonly used methods for
67 measuring bioaccessibility are DIN method (RUB, Germany), In Vitro Digestion model (RIVM,
68 The Netherlands), Physiologically Based Extraction Test (PBET), SHIME, LabMET/Vito,
69 Belgium, Simplified Bioaccessibility Extraction Test (SBET) , etc. Difference in the
70 bioaccessibility method can lead to difference in the value of the bioaccessible concentrations also,
71 as the contaminant concentration released during a particular method depends on : (1) the pH of the
72 gastrointestinal compartment, (2) the residence time of the soil in the solution, (3) the pH of the
73 small intestinal solutions, (4) the ratio of solid to liquid in the gastric solution, (5) different bile
74 concentrations and the different bile salts. These factors has been explained in detail in (Oomen et
75 al., 2002). Owing to the different procedures and the results obtained the unified BARGE method
76 (UBM) was developed by the Bioaccessibility Research Group of Europe (BARGE) for measuring
77 the oral bioaccessibility of contaminants in order to harmonize the use of oral bioaccessibility in

78 contaminated soils of Europe The UBM method was used for the oral bioaccessibility evaluation in
79 the present study as : (1) the method has been validated against in vivo studies for As, Cd and Pb
80 (Denys et al., 2012) and (2) Hamilton et al. (2015) used the method to evaluate oral bioaccessibility
81 of BGS 102 reference material and provided guidance data on a wider range of chemical elements
82 making it feasible to control the quality of the data produced as the variations in the results can be
83 checked due to inter-laboratory trials. Many studies have used the UBM method to assess
84 contamination due to PTE in mining affected areas. For example, Pelfrêne et al., (2012) quantified
85 bioaccessible concentrations of Cd, Pb and Zn as 78%, 32%, and 58% respectively on smelter-
86 contaminated agricultural soils in a coal mining area of northern France. Foulkes et al., (2017)
87 applied the UBM method to measure bioaccessibility of Pb, Th, and U on solid wastes and soils
88 from an abandoned uranium mine site in South West England. However, in Italy there is little to no
89 attention towards inclusion of oral bioaccessibility in studies reporting HHRA (Kumpiene et al.,
90 2017). Consequently, the present study provides evidence towards evaluating bioaccessibility to
91 support the HHRA procedures for two abandoned mine sites in Italy.

92 Potentially toxic elements (PTE) are associated with the various components in EW and
93 soils in different ways, and these associations can lead to variation in both mobility and availability
94 (Cipullo et al., 2018). A wide range of EW and soil properties can thus lead to variation in
95 bioaccessibility of PTE such as pH, organic matter content, presence of clay, iron oxides and
96 alumino-silicates (Ruby et al., 1999; Peijnenburg and Jager, 2003; Martin and Ruby, 2004; Basta
97 et al., 2005; Palumbo-Roe and Klinck, 2007; Denys et al., 2009; Reis et al., 2014; Palumbo-Roe et
98 al. 2015). Therefore, determining the soil-phase fractionation in the matrix can be used as
99 additional line of evidence to the in vitro bioaccessibility testing. Sequential selective chemical
100 extractions are widely used for characterizing the distribution of elements in the solid phase (Li et
101 al., 2001). However, a number of limitations are often associated with sequential chemical
102 extraction schemes., most commonly, the difficulty of finding a suitable method for all soil types
103 and elements. Cave et al. (2004) proposed a non-selective method coupled to chemometric analysis

104 that is called chemometric identification of substrates and element distributions (CISED). The main
105 advantages of CISED method are simplicity of extraction procedure, and the partitioning of the
106 chemical elements between the different components is not methodologically defined. The CISED
107 is a useful methodology for understanding the results provided by in vitro bioaccessibility tests
108 (Palumbo-Roe and Klinck, 2007; Cox et al., 2013).

109 The bioaccessibility of PTE has also been known to be affected by mineral phases present in
110 matrices of EW and soil. The PTE bioaccessibility in comparison to the total concentrations has
111 been known to be constrained by mineralogical aspects such as : (1) encapsulation of PTE in the
112 mineral matrices which leads to changes in PTE-bearing surface area and (2) the association of PTE
113 with different type of minerals resulting into formation of alteration products. Therefore, in order to
114 assess the bioaccessibility of PTE and understanding factors influencing bioaccessibility it is
115 imperative that we study geochemical data and mineral phases present in EW and soil. Considering
116 the challenges linked with evaluating bioaccessibility and, the present study focuses on extractive
117 waste (EW) and soils from the abandoned mine site at Campello Monti, which was important for Ni
118 exploitation from mafic formations in north-west Italy. The study is structured on five main
119 sections: (1) measuring total concentrations of PTE, (2) assessing bioaccessibility of PTE using
120 UBM, (3) determining solid phase distribution of elements in different components using CISED,
121 (4) mineralogical analysis of soil samples and (5) relating bioaccessible concentrations and
122 mineralogy and geochemistry of EW and soil samples.

123

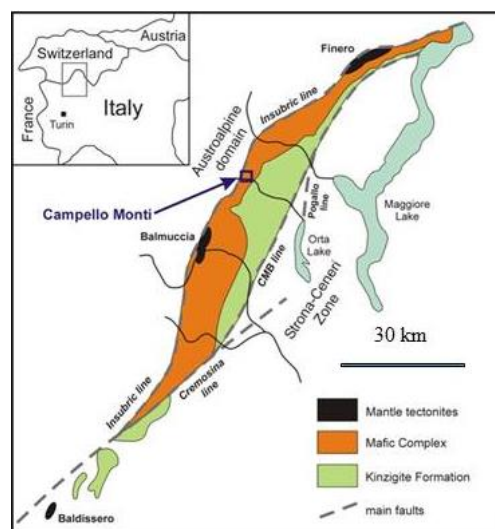
124 **2. Methodology**

125 **2.1 Site description**

126 Campello Monti is a small settlement in the village of Valstrona in the northern sector of Piemonte,
127 Italy. Geologically, the site (**Figure 1**) is present in the ultramafic layers of the mafic complex of
128 the Ivrea Verbano Zone. The Ivera- Verbano zone is a tectonic unit which has preserved the
129 transition from amphibolite to granulite facies (Redler et al., 2012). The mafic formation consists of

130 a sequence of cumulate peridotites, pyroxenites, gabbros and anorthosites, together with a large,
131 relatively homogeneous body of gabbro-norite, grading upwards into gabbro-diorite and diorite.
132 The Campello Monti area consists of lherzolites, in places with titanolivin, in large and smaller
133 masses.

134 The rocks in this area are rich in nickel, copper and cobalt. The area was exploited for nickel
135 production from Fe-Ni-Cu-Co magmatic sulfide deposits occurring from the Sesia to Strona valleys
136 from the 19th Century (1865) until the 1940s. The ore was extracted using underground mining
137 activities that left waste rocks near the mine tunnels (Mehta et al., 2018).

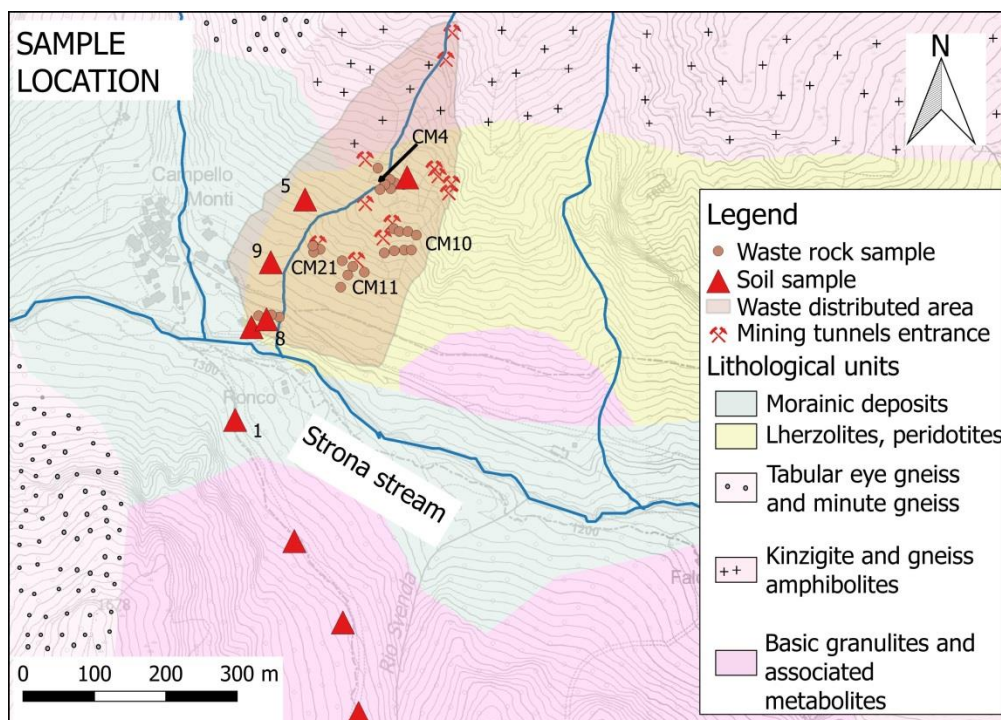


138
139 Figure 1. Geological setting of Campello Monti (modified from Fiorentini and Beresford, 2008).

140 2.2 Sample collection and preparation

141 A site investigation was performed to collect information about waste typology and location, in
142 order to ensure that the facilities are suitable for characterisation and sampling. The sampling site at
143 Campello Monti is composed of different waste rock dumps. These waste rock dumps were placed
144 on the north of the Strona stream and were formed by the dumping in vertical sequence of non-
145 valuable mineralisations and non-mineralised rocks. A systematic sampling strategy was adopted in
146 order to obtain representative data of the whole waste facility. Waste rock material was sampled
147 using hand shovel and a hammer (where necessary). Each sample (8-10 kg) was collected in an area

148 of 1.5 m², by mixing 4 subsamples present at the vertices of the square and one subsample at the
 149 centre of the square. after removing organic residues. In total, 26 samples of waste rock were
 150 collected at the site in July 2016 (**Errore. L'origine riferimento non è stata trovata.**). Additionally, a
 151 total of 9 soil samples were taken near the waste rock dumps to the north and south of the Strona
 152 stream during the sampling campaigns in June 2016 and March 2017. In order to obtain
 153 representative soil samples, the samples taken were formed by mixing 4 subsamples taken at the
 154 vertices of a 1m x 1m square. All samples were taken at a depth of 0-15 cm. The extractive waste
 155 samples and soil samples were dried in an oven for a period of 24 h to remove any moisture.
 156 Samples were then sieved through 2 mm sieves and quartered to obtain a representative sample size
 157 of 10 g. The pH was measured in a 1: 2.5 suspension of each sample in water (ISO 10390, 2005).



158
 159 Figure 2. Waste rock and soil sample locations at Campello Monti. Sample numbers are shown for
 160 the samples analyzed for bioaccessibility.

161
 162 **2.3 Total concentrations measurement**

163 The samples were analyzed for their concentrations of chemical elements on the 2 mm fraction
 164 using the method described in U.S. EPA, 3051 A, (2007) and U.S. EPA, 6010 C, (2007). Briefly,

165 0.5 g of sample was digested using 3 ml concentrated HNO₃ and concentrated HCl (1:3). The
166 concentrations of As, Be, Cd, Co, Cr (total), Cu, Ni, Pb, Sb, Se, V and Zn were measured using an
167 Ametek Spectro Genesis Inductively Coupled Plasma-Optical Emission Spectrometer (ICP-OES).
168 The instrument was provided with an Ametek monochromator, a cyclonic spray chamber and a
169 Teflon Mira Mist nebulizer. The instrumental conditions included a plasma power of 1.3 kW,
170 sample aspiration rate of 30 rpm, argon nebulizer flow of 1 l/min, argon auxiliary flow of 1 l/min
171 and argon plasma flow of 12 l/min. All the reagents used were of analytical grade. All metal
172 solutions were prepared from concentrated stock solutions (Sigma Aldrich). High-purity water
173 (HPW) produced with a Millipore Milli-Q Academic system was used throughout the analytical
174 process. All samples were analyzed in duplicate.

175

176 **2.4 Bioaccessibility analysis (Unified BARGE method)**

177 Following the analysis on total concentration of elements for the fraction under 2 mm, samples were
178 selected for the measurement of bioaccessible concentrations. Waste rock and soil samples were
179 selected to ensure representation of each dump and lithology. For tailings, the two samples closest
180 to the ground surface were measured for bioaccessible concentrations. The total metal
181 concentrations were measured on the <250 µm fraction using aqua regia extractions as described in
182 section 2.3. Following the analysis on total concentration of PTE on the <2 mm fraction, samples
183 of waste rock, soil and tailings were selected for measurement of bioaccessible concentrations,
184 ensuring good representation of each matrix. For tailings, the two samples at the nearest depth from
185 the ground were measured for bioaccessible concentrations. Each sample was sieved to <250 µm
186 and total concentrations of PTE were measured using aqua regia extractions as explained in section
187 2.3. The Unified BARGE method (UBM) was also followed for measuring bioaccessible
188 concentrations of the <250 µm fraction (BARGE 2010, Denys et al., 2012). To ensure quality
189 control of the extraction process each batch of UBM extractions (n=10) included one procedural
190 blank, six unknowns, one duplicate of two unknown samples and one soil reference material

191 (BGS102) (BARGE 2010; Hamilton et al., 2015). **Table 1** shows the comparison of the certified
192 and measured values of the BGS 102 extractions. As pH plays an important role in controlling the
193 leaching of the PTE from the matrix and overall extraction process, the pH meter was calibrated
194 before extraction of every batch of samples.

195 Unified BARGE method extractions were carried out using simulated digestive fluids
196 including saliva, gastric fluid, bile and duodenal fluid, which were prepared from inorganic and
197 organic reagents and enzymes one day prior to sample extractions. These fluids were used to
198 represent three main compartments of human digestive system: mouth, stomach and small intestine.
199 The extraction consists of two phases, gastric and gastro-intestinal for which 0.4 ± 0.0005 g of
200 sample was weighed in replicate in polycarbonate tubes (1 replicate for the gastric phase and 1
201 replicate for the gastro-intestinal phase). For gastric phase extractions, saliva and gastric fluids were
202 added to each tube (pH adjusted to 1.2 ± 0.05), followed by 1 h of end-over-end rotation. The
203 rotator was placed in an oven at a constant temperature of 37 °C. One of the replicates was
204 extracted through centrifugation at 4500 g for 15 min (G phase), while the second replicate was
205 retained for gastro-intestinal phase (GI phase) extraction. Simulated duodenal and bile fluids were
206 added to this tube (pH adjusted to 6.3 ± 0.5) and rotated end-over-end for 4 hours at 37 °C. This
207 was followed by an identical centrifugation procedure to obtain GI phase extracts. For both
208 extractions, 10 ml of the supernatant was collected and preserved with 0.2 ml concentrated (15.9 M)
209 HNO₃. Determination of PTE was performed by ICP-MS (Perkin-Elmer NexION 350X), while
210 using an internal standard (Rh). The bioaccessible fraction (BAF) for both the phases was
211 calculated using Equation 1. To apply a conservative approach for human health risk assessment,
212 BAF is reported as the percentage of highest bioaccessible concentration from gastric or gastro-
213 intestinal phase.

214

$$215 \text{ BAF} = \frac{\text{Concentration of bioaccessible element } \left(\frac{\text{mg}}{\text{kg}}\right)}{\text{Total concentration of element } \left(\frac{\text{mg}}{\text{kg}}\right)} \times 100 \quad (1)$$

216

217 **2.5 Chemometric identification of substrates and element distribution (CISED)**

218 A non-specific sequential nitric acid extraction (Cave et al., 2004) was carried out on selected
219 samples (n=5) (n=2 waste rocks, n=3 soil). Briefly, 2 g of sample was sequentially extracted with
220 10 ml of deionized water and a solution of increasing concentration of HNO₃ ranging from 0.01 M
221 to 5.0 M. A total of 7 solutions were used twice (0.0 M, 0.01 M, 0.05 M, 0.1 M, 0.5 M, 1.0 M and
222 5.0 M), with progressive addition of H₂O₂ (0.25, 0.50, 0.75, and 1 ml) in the last 4 extracting
223 solutions to facilitate the precipitation of oxides. Each solution was mixed for 10 min in an end-
224 over-end shaker and centrifuged (4350 g for 5 min) to separate solid and liquid fractions. The solid
225 fraction was then resuspended in the following extracting solution. The recovered liquid fraction
226 was filtered with a 0.45 µm 25 mm nylon syringe filter and diluted 4 times with deionized water
227 prior to analysis. Extracts were spiked with internal standards (Sc, Ge, Rh, and Bi) and the
228 following elements Ca, Fe, K, Mg, Mn, Na, S, Si, P, Al, As, Ba, Cd, Co, Cr, Cu, Hg, Li, Mo, Ni,
229 Pb, Sb, Se, Sr, V, Zn were measured using ICP-MS (NexION® 350D ICP-MS, Perkin Elmer). For
230 data quality control, acid blanks (1% nitric acid) and certified reference material (BGS102) were
231 included in the extraction procedure.

232

233 **2.6 Modelling**

234 Solid phase distribution of elements in soil and waste rock was calculated with MatLab (MatLab®
235 Version R2015a) using a self-modelling mixture resolution algorithm (SMMR) developed by Cave
236 et al. (2004). This modelling algorithm was used to identify (1) soil components with similar
237 physical-chemical properties, (2) chemical composition data (single elements in each soil
238 component expressed as percentage), and (3) amount of elements in each component (expressed in
239 mg/kg). The algorithm was run separately for waste rock and soil producing 7 and 8 distinct sets of
240 physico-chemical phases for each of these respective runs. In order to categorise these physio-
241 chemical phases into common distinct soil phases hierarchical clustering was used in combination
242 with geochemical profile interpretations. Briefly, heatmaps from hierarchical clustering were

243 produced with a mean-centered and scaled matrix of profile and composition data using the Ward's
244 method in R (v.3.4.1) and the results obtained were plotted with ggplot2, reshape2, grid and
245 gg dendro packages (Wickham,2007; Wickham, 2009; Chang et al. 2013).

246

247 **2.7 Mineralogical analysis**

248 The mineralogical analysis of waste rock samples was performed in a previous study (Rossetti et
249 al., 2017). Consequently, only the soil sample was analyzed for mineral phases in the present study.
250 Micro-X-ray fluorescence (micro-XRF) was used to identify crystalline phases in the bulk soil
251 sample (sample code - 8). Element X-ray maps of soil samples were acquired using a micro-XRF
252 Eagle III-XPL spectrometer equipped with an EDS Si(Li) detector and with an EdaxVision32
253 micro-analytical system. The operating conditions were 2.5 μ s counting time, 10 kV accelerating
254 voltage and a probe current of 20 μ A. The spatial resolution was about 65 μ m in both x and y
255 directions. The elemental maps were processed to determine mineral phases in soil using software
256 program Petromod (Cossio et al., 2002). The micromorphology and associated chemical analysis of
257 solid phases in soil were analyzed with a Cambridge Stereoscan 360 scanning electron microscope
258 (SEM) equipped with an energy-dispersive spectrometry (EDS) Energy 200 system and a Pentafet
259 detector (Oxford Instruments). 10 kV accelerating voltage and 50 s counting time were used for
260 analysis of the minerals. SEM-EDS quantitative data (spot size 2 μ m) were acquired and processed
261 using the Microanalysis Suite Issue 12, INCA Suite version 4.01; natural mineral standards were
262 used to calibrate the raw data; the $\phi\rho Z$ correction (Pouchou & Pichoir, 1988) was applied. Absolute
263 error is 1 δ for all calculated oxides.

264

265 **3. Results**

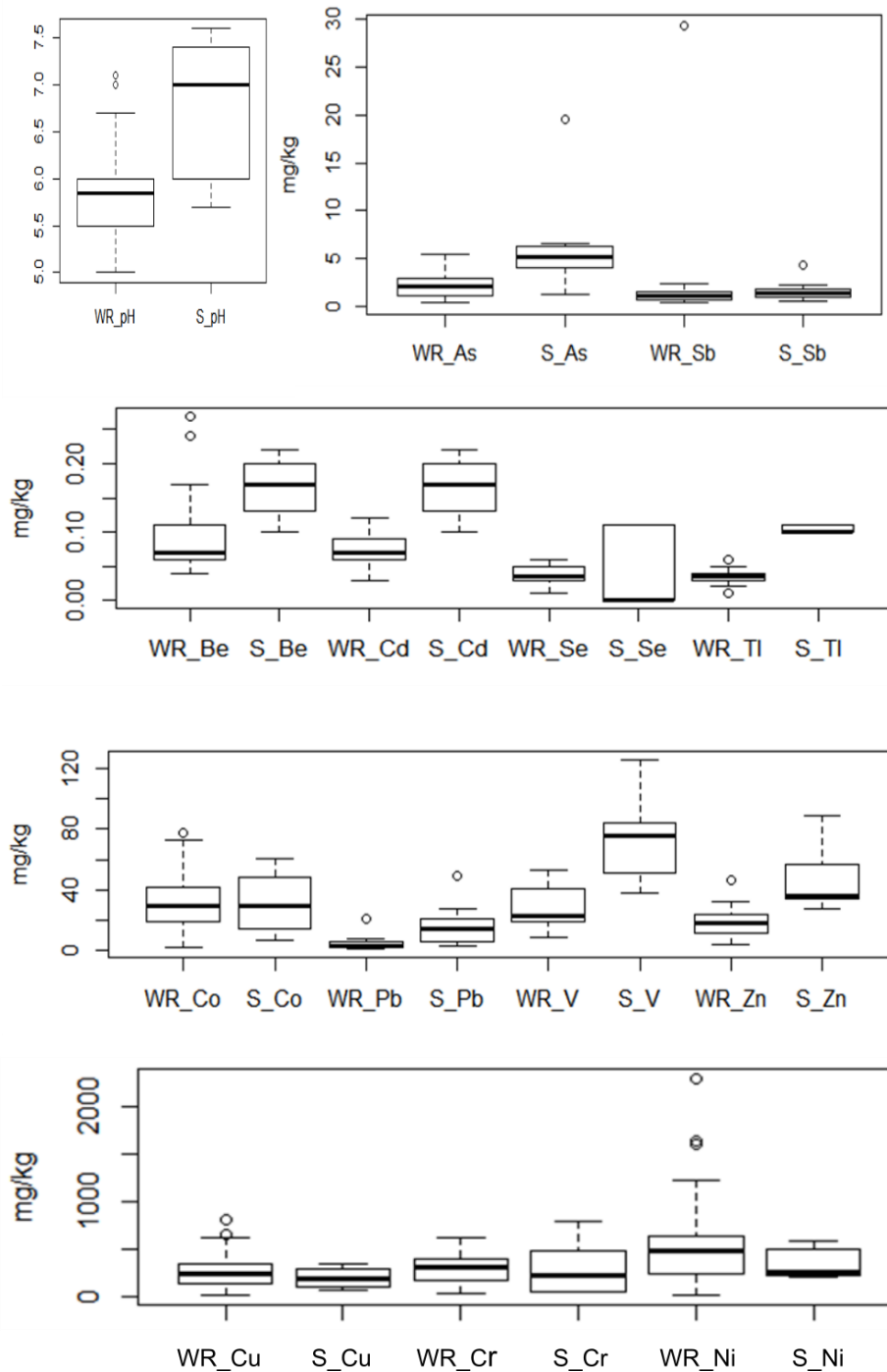
266 **3.1 Total concentrations of PTE**

267 The pH and total concentrations of PTE in waste rock samples (no. of samples, n = 26) and soil
268 samples (no. of samples, n = 9) are summarized in **Figure 3**. The value of pH varied from 5.0 to 7.1

269 with a mean value of 5.9. The results showed that concentrations of Ni varied from 15.2 mg/kg to
270 2294 mg/kg with an average concentration of 640 mg/kg. The presence of slightly acidic samples
271 and high concentrations of Ni can be attributed to the presence of ultramafic lithology rich in
272 olivine and pyroxene in Campello Monti.

273 The concentration of Cr varied from 39 mg/kg to 620 mg/kg with an average concentration
274 of 299 mg/kg, while concentrations of Co ranged from 2.4 mg/kg to 77.8 mg/kg with a mean
275 concentration of 32.1 mg/kg. The presence of Cr and Co is due to the fact that Ni in earth's crust
276 exhibits chalcophile and lithophile characteristics and is found to be associated with Cr and Co.
277 Copper was found to vary from 19 mg/kg to 806 mg/kg with a mean concentration of 284 mg/kg.
278 The presence of Cu suggests that sulfide rich minerals (e.g. pyrite and chalcopyrite) that host both
279 Ni and Cu, may be present at the site. It should be noted that concentrations of Ni, Cr, Co and Cu in
280 waste rocks are higher than Italian permissible limits for soils for recreational and habitation areas
281 (Ministero dell'ambiente e della tutela del territorio, 2006, decree no. 152/06).

282 Analysis of soil samples showed that pH values ranged from 5.7 to 7.6 with an average
283 value of 7.0. The samples were found to be in near neutral conditions and less acidic than waste
284 rock samples. Total Ni, Cr and Cu ranged from 212 to 594 mg/kg, 46 to 795 mg/kg and 66 to 345
285 mg/kg respectively. Mean Ni, Cr, Cu concentrations, were 347, 296 and 200 mg/kg, an order of
286 magnitude above the Italian permissible limits for soils for recreational and habitation areas.
287 Concentrations of V were found to vary from 38 mg/kg to 126 mg/kg with a mean concentration of
288 72 mg/kg. Concentrations of other elements were found to be within permissible limits. The
289 presence of PTE in soil can be explained on the basis of lithogenic origin of soils and possible
290 transport of PTE from extractive waste dumps.



291

292 Figure 3. Box and Whisker plots showing pH and concentration of PTE in mg/kg in waste rock
 293 (n=26) and soil samples (n=9) on <2 mm size fractions at Campello Monti. pH and elements on X-
 294 axis are provided with sample identification code WR for waste rocks and S for soil samples.
 295

296 3.2 Bioaccessible concentrations

297 The total and bioaccessible concentrations of As, Cd, Co, Cr, Cu, Ni, Pb and V in waste rock and
 298 soil samples at Campello Monti are presented in **Table 2**. Total concentrations for the <250 µm size

299 fraction were considerably higher than total concentrations for size fractions under 2 mm (reported
300 in Figure 3) potentially due to an increase in surface area and thus higher the absorption of PTE to
301 particles (Yao et al., 2015). The bioaccessible concentrations were measured both for
302 gastrointestinal and gastric phases. It was observed that for all PTE except As, metals were more
303 bioaccessible in the gastric phase than the gastrointestinal phase. The bioaccessible fraction (BAF)
304 was calculated as the ratio of the higher value of bioaccessible concentration (either gastric or
305 gastrointestinal) to total concentration. The highest bioaccessibility value is used to ensure
306 conservative values are used during risk assessment.

307 Total concentrations of As in waste rock and soil samples varied from 5.6 to 11.1 mg/kg and
308 from 8.8 to 39.3 mg/kg respectively. The bioaccessible concentrations in gastrointestinal phase in
309 waste rock and soil samples varied from 0.6 to 1 mg/kg and from 1.8 to 2.7 mg/kg respectively.
310 Mean values of BAF were found to be 10.5% for waste rock samples and 12.8% for soil samples.
311 Waste rock and soil samples showed mean total concentrations of Cd as 1.3 mg/kg and 0.5 mg/kg.
312 The bioaccessible fractions were found to vary from 3% to 19% and from 20% to 85%, for waste
313 rocks and soil, respectively.

314 Total concentrations of Co in waste rock and soil samples varied from 165 to 266 mg/kg and
315 from 45 to 175 mg/kg respectively. The bioaccessible concentrations in waste rock and soil samples
316 varied from 27 to 72 mg/kg and from 5 to 53 mg/kg respectively. Mean values of BAF were found
317 to be 20% for waste rock samples and 26% for soil samples. The results on Co bioaccessibility
318 showed that although total concentrations of Co were very less in comparison to Cr, the
319 bioaccessible concentrations were present in the same range as Cr due to higher bioaccessible
320 fractions of Co in comparison to Cr. Chromium in waste rock and soil samples was found to vary
321 from 931 to 1569 mg/kg and from 79 to 1643 mg/kg respectively. Mean values of BAF of Cr for
322 waste rock and soil samples was 1% and 2.75% respectively.

323 Total concentrations of Cu in waste rock and soil samples ranged from 953 to 2,006 mg/kg
324 and from 85 to 848 mg/kg respectively. The bioaccessible concentrations in waste rock and soil

325 samples varied from 129 to 921 mg/kg and from 27 to 222 mg/kg respectively. Mean values of
326 BAF were found to be 31% for waste rock samples and 26% for soil samples. Copper results
327 showed higher bioaccessibility for soil samples compared to waste rocks, indicating a contrasting
328 behavior with respect to the other PTE analysed. The results of Cu bioaccessibility showed that
329 although total concentrations of Cu were not as high as Ni, the bioaccessible concentrations were
330 almost of the same magnitude as nickel. This can be attributed to the higher BAF values of Cu
331 when compared with Ni.

332 The samples were found to have a very high total concentration of Ni in waste rock samples
333 with a variation from 1181 to 7408 mg/kg. However, the bioaccessible concentrations of Ni in
334 gastric phase for waste rock samples was relatively low. The bioaccessible concentrations for
335 gastric phase for Ni varied from 119 to 776 mg/kg for waste rock samples, thus leading to a BAF
336 (ratio of bioaccessible concentration to total concentration) of approximately 10%. A similar
337 observation was made for soil samples. The total concentration and bioaccessible concentration for
338 soil samples ranged from 59 mg/kg to 1504 mg/kg and from 12 to 280 mg/kg, respectively, thus
339 leading to BAFs varying from 5% to 20%.

340 Mean values of total concentration of Pb in waste rock and soil samples were found to be 25
341 mg/kg and 18 mg/kg respectively. The bioaccessible fraction of Pb in waste rock and soil samples
342 varied from 42% to 61%. Vanadium was found to vary from 34 mg/kg to 87 mg/kg for waste rock
343 samples, with mean BAF of 4%. The soil samples recorded mean values of total concentrations and
344 bioaccessible concentrations as 106 mg/kg and 7 mg/kg respectively.

345 The range of bioaccessibility values reported for the soils were found to be comparable to
346 those reported elsewhere, eg. Barsby et al. (2012) conducted bioaccessibility analysis in ultramafic
347 geological setting of Northern Ireland using UBM and reported mean values of gastric phase of
348 BAF of As, Co, Cr for soils as 14%, 18% and 1% respectively (here 13%, 26% and 3%
349 respectively). The same study reported mean values of BAF for Cu as 31 % (here 31%), Ni as 12%
350 (here 13%), V as 9% (here 7%). There was a marked difference in reported values of mean of BAF

351 of Pb as reported by Barsby et al. (2012) 33% (here 54%). However, the value was found to be
352 more comparable with smelter contaminated agricultural soil of northern France, which showed a
353 BAF of 58% (here 54%) (Pelfrêne et al., 2012).

354

355 Table 1. Results of the UBM digests of certified reference material BGS 102 (n=3).

		As	Cd	Co	Cr	Cu	Ni	Pb	V
Gastric phase	Measured	3.17 ± 0.13	BDL ^b	9.57 ± 0.61	35.76 ± 0.58	8.66 ± 0.69	12.70 ± 0.51	15.35 ± 1.16	6.67 ± 0.40
	Reported ^a	3.90	0.02	9.50	36.70	8.60	13.00	15.30	6.10
Gastro-intestinal phase	Measured	2.54 ± 0.38		5.70 ± 0.75	6.19 ± 1.06	9.86 ± 0.82		2.23 ± 0.46	
	Reported	3.30		5.50	13.10	10.50		3.40	

356 ^aHamilton et al., 2015; ^bBDL- Below detectable limit.

357

358 Table 2. Total concentrations (mg/kg), bioaccessible concentrations (G and GI) (mg/kg) and BAF (%) measured on <250 µm size fractions for
359 samples at Campello Monti.

	Sample	As			Cd			Co			Cr		
		GI	total	BAF	G	total	BAF	G	total	BAF	G	total	BAF
Waste rock	CM4	0.6	5.6	11	0.1	0.9	6	27	188	14	25	1398	1
	CM10	1	11.1	9	0.3	1.4	19	69	266	26	20	1569	1
	CM11	0.6	7.5	9	0.2	1.9	13	58	295	20	26	1296	1
	CM21	0.7	6.3	13	0.0	1.1	3	30	165	18	9	931	1
Soil	5	1.8	15.3	11	0.2	1.0	20	53	175	31	54	1643	1
	1	2.9	39.6	7	0.6	0.7	85	23	68	34	3	79	3
	8	1.8	8.8	22	0.1	0.2	47	37	142	26	85	623	1
	9	1.2	9.4	12	0.2	0.2	73	5	45	10	124	701	6
	Sample	Cu			Ni			Pb			V		
		G	total	BAF	G	total	BAF	G	total	BAF	G	total	BAF
Waste rock	CM4	129	953	14	119	1181	10	10	21	49	2	87	2
	CM10	754	1955	39	502	4586	11	12	24	50	2	64	3
	CM11	921	2006	47	776	7408	10	10	25	42	2	34	6
	CM21	320	1367	23	256	2864	9	14	28	50	2	61	3
Soil	5	222	848	26	280	1504	19	8	15	51	9	149	5
	1	27	85	32	12	59	21	29	49	59	5	94	6
	8	135	441	31	73	1455	5	2	4	44	3	79	4
	9	45	256	17	38	763	5	2	4	61	12	101	12

360 G = gastric phase and GI = gastrointestinal phase of UBM. Total represents total concentration of PTE using *aqua regia*. Bioaccessible fraction is
361 represented as BAF.

362 3.3 Interpretation of sequential extraction data

363 Identified physico-chemical components for the most representative samples of waste rock (sample
364 code - CM 10) and soil (sample code - 8) at Campello Monti are highlighted in **Figure 4**. For these
365 samples, the chemometric data analysis identified 7 components in the waste rock sample and 8
366 components in the soil sample. Each row represents a component identified by the algorithm, where
367 the name is composed of the elements that make up >10% of the composition. The columns of the
368 heatmap are based on model output showing the composition (%) on the left side, and on the right
369 side the extraction profiles (E1-E14).

370 A combination of geochemistry knowledge, relative solubility of each component in the
371 extracts, major elemental composition, profile, and clustering obtained from the heat maps were
372 used to define 6 geochemically distinct clusters: pore-water, exchangeable, Fe oxide 1, clay related,
373 Fe oxide 2. The heatmap and clustergram for the remaining waste rock and soil samples are shown
374 Supplementary Material (Figure 1).

375

376 Pore-water: In waste rock, the pore-water cluster was principally made up of S (*c.* 52.2%) and Mg
377 (*c.* 24.7%). Other elements extracted were Ca (*c.* 7.4%) and Ni (*c.* 8.8%). The presence of nickel in
378 the pore water component suggests mobility of Ni in the waste rock. The pore-water cluster of soil
379 was predominantly composed of S (*c.* 64%) and Na, Mg, K which were all present at >5 %. These
380 components in this cluster were extracted in water extractions and 0.01 M HNO₃ (E1-E4). This was
381 the most easily extracted cluster suggesting it could be associated with the residual salts from the
382 original pore water in the soil.

383

384 Exchangeable: In waste rock, the exchangeable component consisted of Cu (*c.* 36%), Mg (*c.* 17 %),
385 S (*c.* 12%) and Ca (*c.* 12%). It was removed by the HNO₃ extracts over the range 0.01 M to 0.05 M.
386 The presence of a Cu rich component could be due to the presence of Cu bearing ores, such as Cu
387 Fe sulfides (chalcopyrite, CuFeS₂ and cubanite, CuFe₂S₃) at the site. The exchangeable cluster of

388 soil was principally composed of Al (*c.* 48%), Ca (*c.* 27%), Cu (*c.* 7%) and S (*c.* 5%). It was
389 removed by the HNO₃ extracts over the range 0.01 M to 0.1 M. High Ca and Al concentrations
390 combined with removal on addition of relatively weak acid suggests that this cluster was associated
391 with the presence of K-feldspar, which was found in micro-XRF analysis of the soil samples.

392

393 Clay related: This cluster was found only in soil and consisted of 4 different components extracted
394 (Al-Si, Al-Si1, Al-Si2, Al-S). It was dominated by Al (*c.* 62%) and Si (*c.* 34%) and to a lesser
395 extent by Fe (*c.* 3%). This component also consisted of the highest % of Co, Cr and Cu released
396 during CISED extractions. These components were extracted with acid concentrations from 0.01 M
397 HNO₃ to 1 M HNO₃, however, most elements were extracted in a narrower band of acid
398 concentrations ranging from 0.1 M HNO₃ to 1 M HNO₃ (E7-E12). The high acid strength for
399 extraction, predominance of Al, Si and Fe, along with presence of trace elements in this cluster are
400 likely to be extracted from clay related minerals and from the primary soil forming minerals such as
401 olivine and pyroxene (Wragg 2005). Clay like minerals such as montmorillonite and kaolinite were
402 identified during mineralogical analysis of soil sample using micro-XRF.

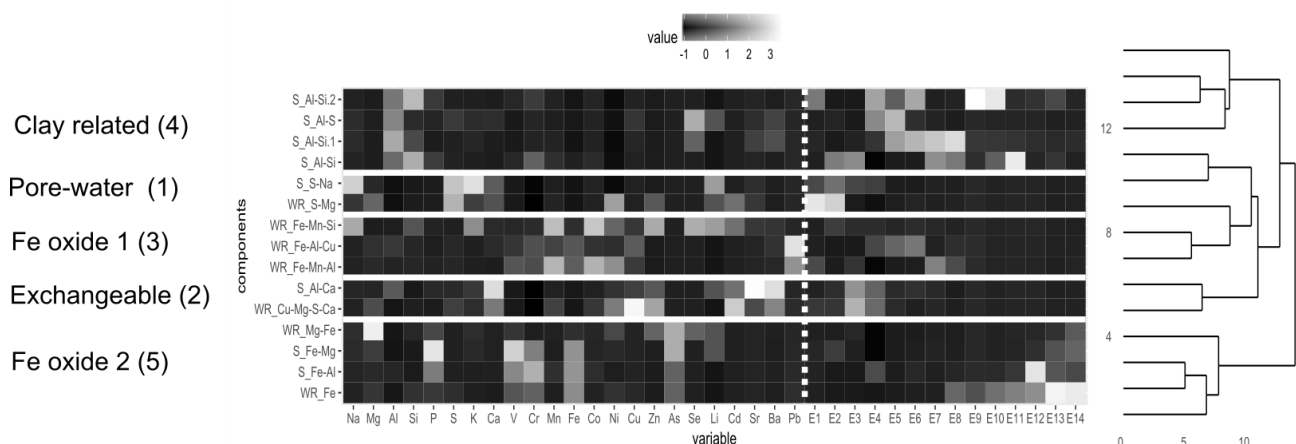
403

404 Fe oxide 1: The Fe oxide cluster was extracted only in waste rock. This cluster consisted of three
405 different Fe dominated components (Fe-Mn-Si, Fe-Al-Cu, Fe-Mn-Al). These Fe dominated
406 components were removed by acid concentrations ranging from 0.05 M HNO₃ to 0.5 M HNO₃ (E5-
407 E10). The important elements extracted were Fe (*c.* 39%), Al (*c.* 16%), Mn (*c.* 12%), Cu (*c.* 7%), Ni
408 (*c.* 6%) and Si (*c.* 6%), Mg (*c.* 5%). The presence of Fe, Cu, Ni rich components can be due to the
409 presence of minerals like Fe Ni sulphide (pentlandite, (Fe,Ni)₉S₈) and Cu Fe sulphide (chalcopyrite,
410 CuFeS₂), which were found in mineralogical analysis of waste rocks from this site (Rossetti et al.,
411 2017). The presence of Al and Si in this Fe oxide cluster showed that in waste rock, both these
412 elements are more closely associated with iron unlike the soil sample, where Al was extracted in the
413 clay related cluster.

414

415 Fe oxide 2: In the waste rock sample, the Fe oxide cluster was principally composed of Fe (c. 65%).
416 Other elements extracted were Al, Mg, Ni, Si, S with varying concentration from 2.6% to 12%. It
417 was removed by the HNO₃ extracts over the range 0.5 M to 5 M (E9-E14). The presence of Fe,S
418 rich components could be due to presence of Fe sulphide mineral (pyrrhotite, Fe_(1-x)S) observed in
419 microscopic images of waste rock from this site (Rossetti et al., 2017). The dominance of Fe and
420 high acid extracts required to extract these components could be due to the presence of hematite
421 occurring naturally in the site (Rossetti et al., 2017). The presence of two different Fe containing
422 components for waste rock suggests the presence of different Fe oxide forms (such as amorphous
423 and crystalline), that are being dissolved at different rates (Cave et al. 2004). The Fe oxide cluster in
424 soil included Fe (c. 75%), Al (c. 11%), Mg (c. 6%) and was removed by extracts containing HNO₃
425 over the range 1 M to 5 M and H₂O₂ (E11-E14). The Fe oxide 2 cluster was rich in Fe and Mg
426 which suggests that the important Fe and Mg bearing minerals of the olivine group were mainly
427 extracted at very high acid concentrations. The cluster was also found to have concentrations of As,
428 Cr and Ni.

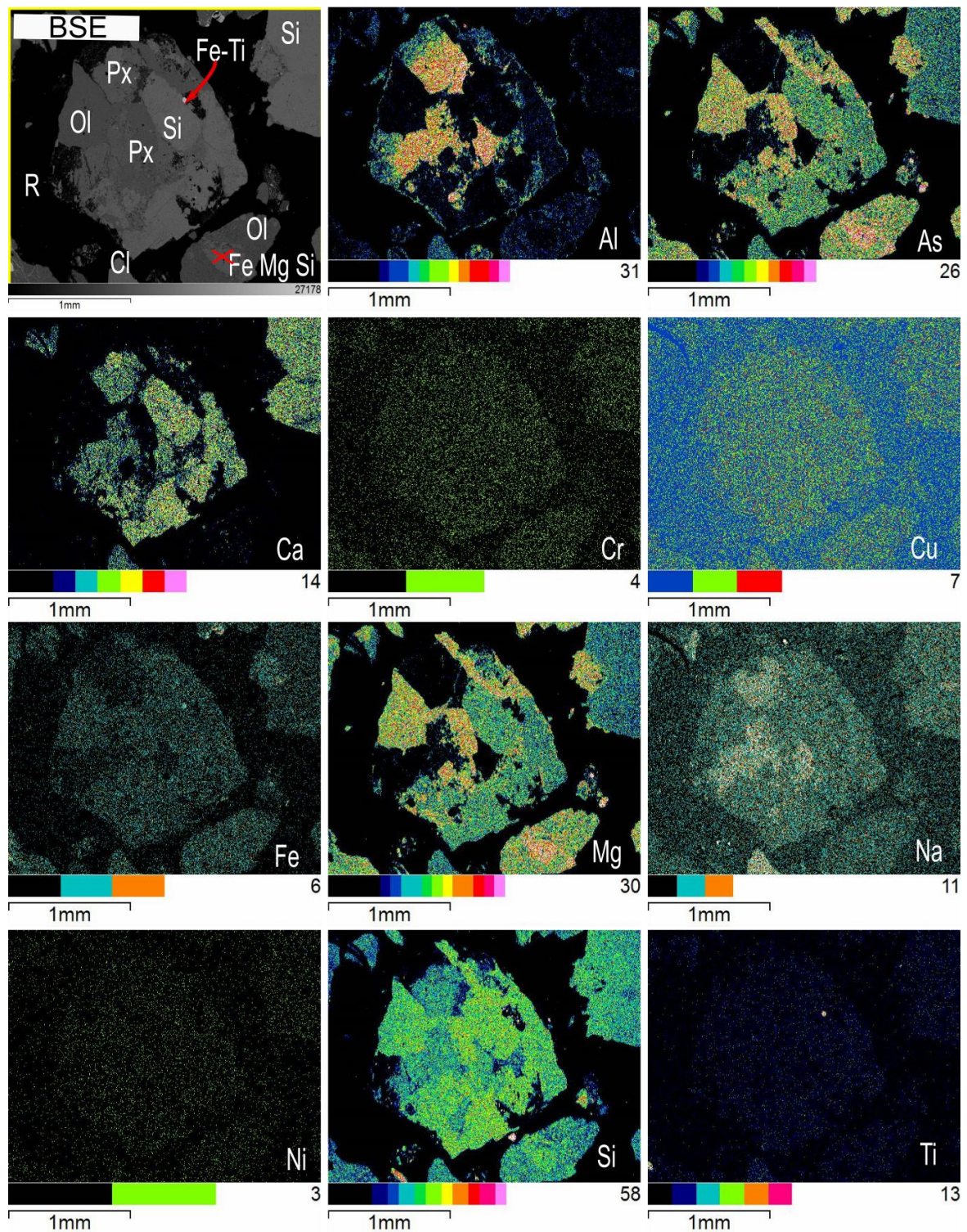
429



430 Figure 4. Heatmap and clustergram for CISED extracted waste rock and soil samples of Campello
431 Monti (CM 10, and soil sample code - 8). The dendrogram on the right-hand side shows how
432 components link together. Elemental composition data is on the left-hand side separated with a
433 dashed vertical white line from the extraction number data (E1–14) on the right. The horizontal
434 white lines divide the map into clusters. High concentrations are depicted by white/light grey and
435 low concentrations by dark grey/black. Component names comprise a sample identification code
436 (WR and S) followed by the principal elements recorded for each component.

437 **3.4 Mineralogical analysis**

438 Semi quantitative analysis using micro-XRF showed that the dominant minerals present in soil
439 (sample code - 8) were clay related (kaolinite and montmorillonite), Fe-Al (Mg) silicates, olivine,
440 plagioclase and pyroxene. The secondary minerals determined during the analysis were Fe oxides,
441 K-feldspar, Mn phases and sulfides. The results from SEM analysis (**Figure 5**) showed that As, Cr,
442 Cu and Ni were locked within mineral grains. Arsenic was present in the minerals that did not
443 contain Al. A reason could be that in primary rock forming silicate minerals, As can be incorporated
444 in minerals through replacement of Al. It was also observed that As occurred in the mineral phases
445 rich in Fe-Mg, showing strong association of As with Fe-Mg in the soil. This was also recorded in
446 CISED analysis of soil samples where As was extracted in very high percentage in the Fe-Mg
447 component. Chromium, Cu and Ni were found to be associated with both Al rich and Fe-Mg silicate
448 minerals.
449



450

451 Figure 5. Detail of elemental distribution and composition of soil (sample code 8) - Back scattered
 452 electron (BSE) image showing Cl : Clay related mineral (montmorillonite), FeMgSi : Fe Mg
 453 silicates, Fe-Ti : Fe-Ti oxide, Ol : Olivine, Px : Pyroxene, R : resin, Si : Ca Mg Fe silicates and
 454 corresponding X-ray maps (SEM) for Al, As, Ca, Cr, Cu, Fe, Mg, Na, Ni, Si and Ti.
 455

456 **3.5 Relation of mineralogy and CISED to bioaccessibility**

457 The extracted PTE and their bioaccessible fraction are plotted in **Figure 6**. The waste rock sample
458 contained 11 mg/kg of As and only 1 mg/kg of this was bioaccessible. The total concentration of As
459 extracted by CISED was also 1 mg/kg, indicating that As extracted in both the methods was similar.
460 80% of total CISED extracted As was associated with the Fe oxide 2 cluster. The Campello Monti
461 site is rich in Fe bearing minerals suggesting that dissolution of Fe oxides/oxyhydroxides took place
462 leading to As in extracted solutions. 9 mg/kg of As was present in the soil sample, while 1.8 mg/kg
463 of this was bioaccessible and 1.2 mg/kg was extracted by CISED, suggesting that As could be
464 present in mineral phases which were not dissolved through CISED but were dissolved in the
465 gastrointestinal phase of bioaccessibility extractions. In fact, the SEM analysis of soil samples
466 confirmed that As was locked in mineral phases of soil samples. Higher dissolution of As enclosed
467 in mineral grains during UBM than CISED could be due to the presence of organic reagents, body
468 temperature conditions and/or the longer reaction time for UBM solutions. In fact, Yunmei et al.
469 (2004) found that during dissolution of Fe-As-S rich mineral assemblages the concentration of As
470 in solution tends to increase with increase in temperature and time.

471 The total concentration of Cu in waste rock was 1955 mg/kg while only 650 mg/kg of Cu
472 (35%) was extracted by CISED extractions. Similar observations were made for Cu present in soil
473 where 33% of Cu was removed in CISED extractions with total concentration and total CISED
474 extracted concentrations of 441 mg/kg and 135 mg/kg, respectively.

475 The bioaccessible concentration of Cu in waste rock was 157 mg/kg resulting in higher
476 bioaccessible Cu concentrations than Cu concentrations recorded during CISED extractions. It
477 suggests that Cu associated with Fe and S present in the Fe oxide 1 cluster, which did not get
478 extracted in CISED extractions, was extracted in bioaccessibility experiments. However, in soil, the
479 bioaccessible concentration was less than the CISED extracted concentration. Bioaccessibility of Cu
480 in soil was due to exchangeable, Fe oxide 2 and dissolution of clay related clusters, while Cu
481 present in the Fe oxide 2 component did not contribute to bioaccessible Cu. The differences in
482 bioaccessible Cu concentrations in waste rock and soil could be due to (a) the association of Cu

483 with metal sulfides in waste rocks while in soil Cu was present in clay related minerals rich in metal
484 silicate phases in soil. It has been found that Cu tends to form a stable and relatively inert complex
485 with Si (Teien et al., 2006), leading to reduction in dissolution in soil compared to waste rock, (b)
486 the difference in ratio of concentration of S/Fe extracted during CISED. It is worth mentioning that
487 the ratio of concentration of S/Fe during CISED extraction in waste rock and soil was 12.8% and
488 7.6% respectively. Studies on dissolution reactions of Cu concluded that Cu is more chalcophile
489 than siderophile and tends to dissolve faster with an increase in ratio of S/Fe in iron-sulfur based
490 solutions (Holzheid and Lodders, 2001).

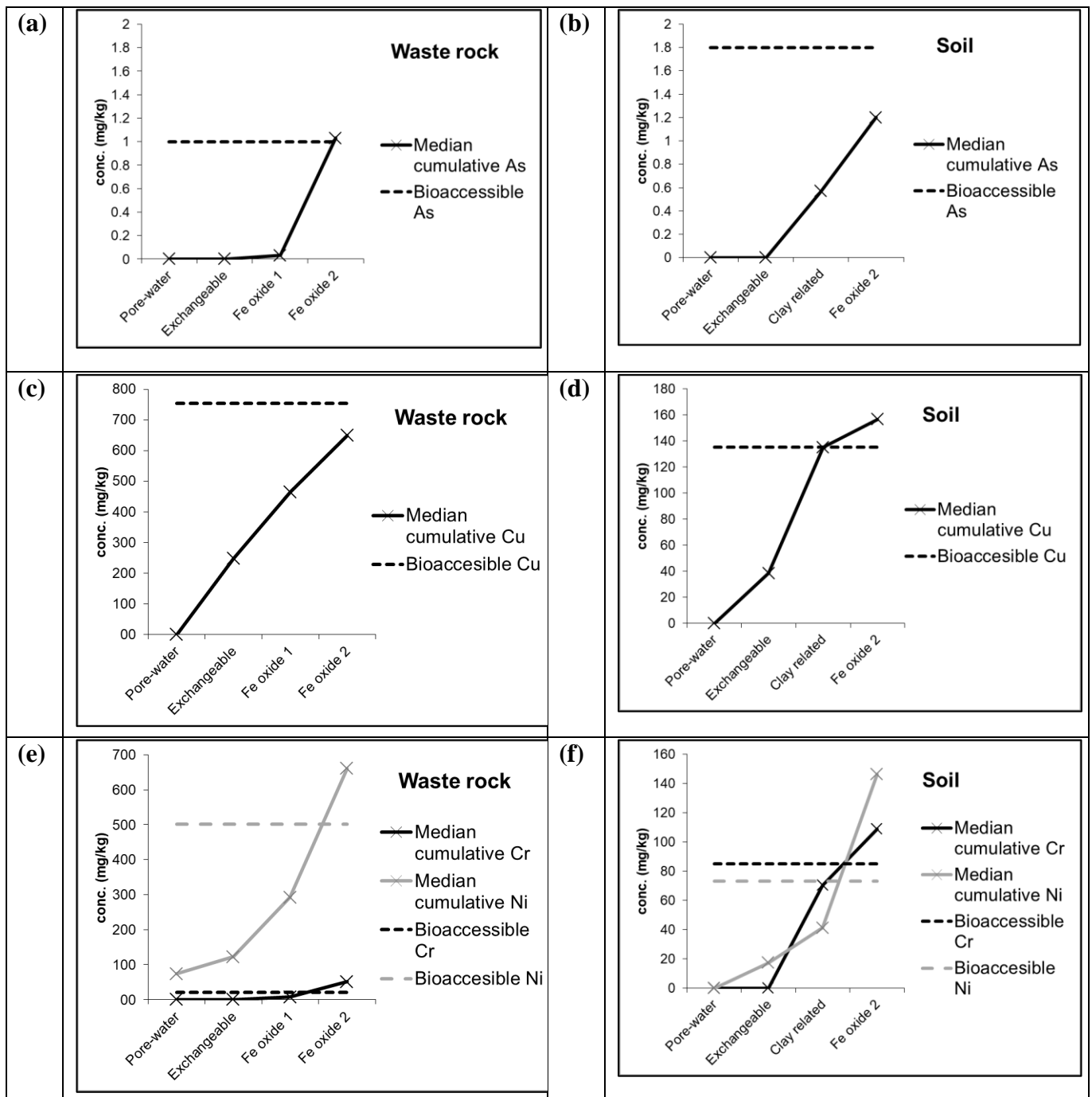
491 In waste rock samples it was observed that the gastric phase bioaccessible concentrations of
492 Cr and Ni increased with increase in total concentration potentially suggesting that the majority of
493 bioaccessible Cr and Ni is derived from phases which contribute to the total Cr and Ni in the sample
494 (Cox et al. 2013). The total concentration of Cr in waste rock was 1,569 mg/kg while 51.2 mg/kg
495 was extracted by CISED. The total concentration of Ni in waste rock was 4,586 mg/kg, however
496 only 661 mg/kg was removed during the CISED procedure. The extraction of 4% of total Cr and
497 14% of total Ni by CISED suggests that the majority of Cr and Ni was present in less reactive
498 minerals such as olivine and pyroxenes that are resistant to attack by HNO₃. Pyroxenes and olivine
499 are present as the primary minerals in the waste rock samples at the site (Rossetti et al., 2017). The
500 source of bioaccessible Cr in the waste rock with the partial dissolution of Fe oxide 2 is shown in
501 Figure 6E. For Ni, it was observed that the same fraction was the source of bioaccessibility, in
502 addition to dissolution of pore-water, exchangeable and Fe oxide 1 components. Higher
503 concentrations of Ni than Cr in pore water and exchangeable components suggests easy dissolution
504 of Ni. It could be because Ni is primarily hosted by olivine in ultramafic rocks. Dissolution of
505 olivine has been found to be rapid in comparison to most silicate minerals as it has a simpler
506 structure (Pokrovsky and Schott, 2000). Venturelli et al. (2016), while studying weathering of
507 ultramafic rocks, found that Ni tends to be more mobile than Cr and was found in higher
508 concentrations in weathered rocks. Another study reporting Cr and Ni mobility concluded that Ni

509 tends to be more readily transferred to secondary minerals (Quantin et al., 2008). Cox et al. (2017)
510 found that Cr concentrations in basaltic soils were related to highly recalcitrant chrome spinel and
511 primary iron oxides, while Ni was more widely dispersed within the soils including in more
512 extractable soil fractions which led to higher BAF measurements being recorded for Ni than Cr.

513 The total concentration of Cr in soil was 623 mg/kg with a bioaccessible Cr concentration of
514 85 mg/kg. The CISED method extracted 108 mg/kg of Cr. Differences in total bioaccessible and
515 CISED extracted concentrations suggest the non-mobile nature of Cr in soil. Dissolution of clay
516 related clusters and partial dissolution of Fe oxide 2 led to the bioaccessible forms of Cr. The total
517 concentration of Ni in soil was 1,455 mg/kg, however only 73 mg/kg was bioaccessible in gastric
518 phase extractions. The bioaccessible form of Ni was likely to come predominantly from the
519 exchangeable and clay related clusters, and to a lesser extent from the Fe oxide 2 cluster, identified
520 by the CISED extraction (**Figure 6e**). The possible reason could be that the clay related cluster
521 consisted of weathered minerals, while the Fe oxide 2 cluster belongs to recalcitrant mineralization
522 at the site in the form of pyrrhotite ($\text{Fe}_{(1-x)}\text{S}$), pentlandite ($(\text{Fe},\text{Ni})_9\text{S}_8$) and chalcopyrite (CuFeS_2)
523 (Rossetti et al., 2017).

524 For As, Cr and Ni it was observed that the BAF was higher for soil samples compared to
525 waste rock samples. This could be because (a) elements in ultramafic lithologies are more tightly
526 bound in the mineral lattice of the waste rocks compared to soils, (b) waste rock samples were more
527 acidic than soil samples, which can cause some PTE to remain immobile (Ruby et al., 1999), (c)
528 elements with particle binding abilities may become immobilised in rocks but can be released
529 during weathering. However, the mean value of bioaccessible fractions in soil for all PTE analyzed
530 was less than 54%. The possible reason could be the embedment of PTE within mineral grains of
531 soil as observed in SEM analysis.

532



533 Figure 6. Median cumulative concentration of elements in different components of CISED
 534 compared with bioaccessible concentrations in samples of Campello Monti (mg/kg).
 535

536

537 4. Conclusions

538 This study investigated total concentrations and bioaccessible concentrations of PTE at an
 539 abandoned mine site of Campello Monti. The results showed that extractive waste facilities and
 540 local soils around the old mining areas are strongly enriched in PTE. This study also provided

541 evidence that total concentrations of PTE were higher in samples with particle size <250 µm
542 compared to samples (<2 mm), due to higher specific surface area in the former case.
543 However, not all of these elements were bioaccessible. The mean value of the bioaccessible fraction
544 (ratio of bioaccessible concentration to total concentration) was observed to be significantly less
545 than 100 % (11%, 1%, and 31% for As, Cr, Cu respectively in waste rocks and 31%, 3%, and 26%
546 for soils). The mean value of BAF of Ni was 10%. Mean values of BAF of V in waste rock and soil
547 were observed to be 4% and 9% respectively. These results show that risk assessment of the site on
548 the basis of total concentrations of PTE alone would significantly overestimate the potential risks to
549 human health at the site.

550 It is clear that the release of PTE and potential risks to human health strongly relies on pH, soil
551 phases, and solubility of Fe-rich phases and presence of clay like minerals. The research conducted
552 highlights how geological and lithological structures together with rock weathering and soil
553 formation processes can lead to variations of bioaccessibility. Traditionally, criteria for the
554 assessment and intervention strategies of contaminated sites have been derived using concentration-
555 based standards and assuming that 100% of the contaminant is bioavailable. However, the results
556 outlined in this research clearly indicate that bioaccessibility evaluations lead to more informed
557 site based risk assessment.

558

559 **Acknowledgements:** This work was completed as part of the REMEDIATE (Improved decision-
560 making in contaminated land site investigation and risk assessment) Marie-Curie Innovation
561 Training Network. The network has received funding from the European Union's Horizon 2020
562 Programme for research, technological development and demonstration under grant agreement n.
563 643087. REMEDIATE is coordinated by the QUESTOR Centre at Queen's University Belfast.
564 <http://questor.qub.ac.uk/REMEDiate/>. Authors will also like to express gratitude towards Jie
565 Chen, Department of Earth Sciences, University of Torino for helping with micro-XRF and SEM

566 analysis. Sincere thanks to Giorgio Carbotta and Prof. Piergiorgio Rossetti, Department of Earth
567 Sciences, University of Torino for helping with sampling and teaching Petromod.

568

569 **References**

570 BARGE (2010). UBM procedure for the measurement of the inorganic contaminant bioaccessibility
571 from solid matrices.

572 Barsby, A., McKinley, J.M., Ofterdinger, U., Young, M., Cave, M.R., and Wragg, J. (2012).
573 Bioaccessibility of trace elements in soils in Northern Ireland. *Sci. Total Environ.* 433, 398–417.

574 Basta, N.T., Ryan, J.A., and Chaney, R.L. (2005). Trace Element Chemistry in Residual-Treated
575 Soil. *J. Environ. Qual.* 34, 49–63.

576 Cave, M. R., Milodowski, A. E., & Friel, E. N. (2004). Evaluation of a method for identification of
577 host physicochemical phases for trace metals and measurement of their solid-phase partitioning in
578 soil samples by nitric acid extraction and chemometric mixture resolution. *Geochemistry:
579 Exploration, Environment, Analysis*, 4, 71–86.

580 Chang, Winston. (2013). *R Graphics Cookbook*. Farnham: O'Reilly.

581 Cipullo, S., Snapir, B., Tardif, S., Campo, P., Prpich, G., and Coulon, F. (2018). Insights into mixed
582 contaminants interactions and its implication for heavy metals and metalloids mobility,
583 bioavailability and risk assessment. *Sci. Total Environ.* 645, 662–673.

584 Cossio, R., Borghi, A. & Ruffini, R. (2002). Quantitative modal determination of geological
585 samples based on X-ray multielemental map acquisition. *Microsc Microanal* 8, 139-149.

586 Cox, S.F., Chelliah, M.C.M., McKinley, J.M., Palmer, S., Ofterdinger, U., Young, M.E., Cave,
587 M.R., and Wragg, J. (2013). The importance of solid-phase distribution on the oral bioaccessibility
588 of Ni and Cr in soils overlying Palaeogene basalt lavas, Northern Ireland. *Environ. Geochem.
589 Health* 35, 553–567.

590 Cox, S.F., Rollinson, G., and McKinley, J.M. (2017). Mineralogical characterisation to improve
591 understanding of oral bioaccessibility of Cr and Ni in basaltic soils in Northern Ireland. *J. Geochem.*
592 *Explor.* *183*, 166–177.

593 Denys, S., Tack, K., Caboche, J., and Delalain, P. (2009). Bioaccessibility, solid phase distribution,
594 and speciation of Sb in soils and in digestive fluids. *Chemosphere* *74*, 711–716.

595 Denys, S., Caboche, J., Tack, K., Rychen, G., Wragg, J., Cave, M., Jondreville, C., and Feidt, C.
596 (2012). In Vivo Validation of the Unified BARGE Method to Assess the Bioaccessibility of
597 Arsenic, Antimony, Cadmium, and Lead in Soils. *Environ. Sci. Technol.* *46*, 6252–6260.

598 Dino, G.A., Mehta, N., Rossetti, P., Ajmone-Marsan, F., and De Luca, D.A. (2018). Sustainable
599 approach towards extractive waste management: Two case studies from Italy. *Resour. Policy.*
600 <https://doi.org/10.1016/j.resourpol.2018.07.009> (in press).

601 Fiorentini, M.L., and Beresford, S.W. Role of volatiles and metasomatized subcontinental
602 lithospheric mantle in the genesis of magmatic Ni–Cu–PGE mineralization: insights from in situ H,
603 Li, B analyses of hydromagmatic phases from the Valmaggia ultramafic pipe, Ivrea-Verbano Zone
604 (NW Italy). *Terra Nova* *20*, 333–340.

605 Foulkes, M., Millward, G., Henderson, S., and Blake, W. (2017). Bioaccessibility of U, Th and Pb
606 in solid wastes and soils from an abandoned uranium mine. *J. Environ. Radioact.* *173*, 85–96.

607 Gál, J., Hursthouse, A., and Cuthbert, S. (2007). Bioavailability of arsenic and antimony in soils
608 from an abandoned mining area, Glendinning (SW Scotland). *J. Environ. Sci. Health Part A* *42*,
609 1263–1274.

610 Golia, E.E., Dimirkou, A., and Mitsios, I.K. (2008). Influence of Some Soil Parameters on Heavy
611 Metals Accumulation by Vegetables Grown in Agricultural Soils of Different Soil Orders. *Bull.*
612 *Environ. Contam. Toxicol.* *81*, 80–84.

613 Hamilton, E.M., Barlow, T.S., Gowing, C.J.B., and Watts, M.J. (2015). Bioaccessibility
614 performance data for fifty-seven elements in guidance material BGS 102. *Microchem. J.* *123*, 131–
615 138.

616 Holzheid, A., and Lodders, K. (2001). Solubility of copper in silicate melts as function of oxygen
617 and sulfur fugacities, temperature, and silicate composition. *Geochim. Cosmochim. Acta* 65, 1933–
618 1951.

619 ISO 10390, 2005. Soil quality – Determination of pH. 7pp, available at
620 <https://www.iso.org/standard/40879.html>.

621 Kumpiene, J., Giagnoni, L., Marschner, B., Denys, S., Mench, M., Adriaensen, K., Vangronsveld,
622 J., Puschenreiter, M., and Renella, G. (2017). Assessment of Methods for Determining
623 Bioavailability of Trace Elements in Soils: A Review. *Pedosphere* 27, 389–406.

624 Li, X., Shen, Z., Wai, O.W.H., and Li, Y.-S. (2001). Chemical Forms of Pb, Zn and Cu in the
625 Sediment Profiles of the Pearl River Estuary. *Marine Pollution Bulletin* 42, 215–223.

626 Lim, M., Han, G.-C., Ahn, J.-W., You, K.-S., and Kim, H.-S. (2009). Leachability of Arsenic and
627 Heavy Metals from Mine Tailings of Abandoned Metal Mines. *Int. J. Environ. Res. Public. Health*
628 6, 2865–2879.

629 Maddaloni, M., Lolocono, N., Manton, W., Blum, C., Drexler, J., and Graziano, J. (1998).
630 Bioavailability of soilborne lead in adults, by stable isotope dilution. *Environ. Health Perspect.* 106,
631 1589–1594.

632 Martin, T.A., and Ruby, M.V. (2004). Review of in situ remediation technologies for lead, zinc, and
633 cadmium in soil. *Remediat. J.* 14, 35–53.

634 Mehta, N., Dino, G.A., Ajmone-Marsan, F., Lasagna, M., Romè, C., and De Luca, D.A. (2018).
635 Extractive waste management: A risk analysis approach. *Sci. Total Environ.* 622–623, 900–912.

636 Ministero dell'ambiente e della tutela del territorio. (2006). *Gazzetta Ufficiale* n. 88 of 14 Aprile
637 2006 Decreto Legislativo 3 aprile 2006, n. 152 "Norme in materia ambientale." (Norms concerning
638 the environment.)

639 Ono, F.B., Penido, E.S., Tappero, R., Sparks, D., and Guilherme, L.R.G. (2016). Bioaccessibility of
640 Cd and Pb in tailings from a zinc smelting in Brazil: implications for human health. *Environ.*
641 *Geochem. Health* 38, 1083–1096.

642 Oomen AG (2000). Determination of oral bioavailability of soil-borne contaminants. University of
643 Utrecht.

644 Oomen, A.G., Hack, A., Minekus, M., Zeijdner, E., Cornelis, C., Schoeters, G., Verstraete, W., Van
645 de Wiele, T., Wragg, J., Rompelberg, C.J.M., et al. (2002). Comparison of Five In Vitro Digestion
646 Models To Study the Bioaccessibility of Soil Contaminants. *Environ. Sci. Technol.* 36, 3326–3334.

647 Palumbo-Roe, B., and Klinck, B. (2007). Bioaccessibility of arsenic in mine waste-contaminated
648 soils: A case study from an abandoned arsenic mine in SW England (UK). *J. Environ. Sci. Health*
649 *Part A* 42, 1251–1261.

650 Palumbo-Roe, B., Wragg, J., and Cave, M. (2015). Linking selective chemical extraction of iron
651 oxyhydroxides to arsenic bioaccessibility in soil. *Environ. Pollut.* 207, 256–265.

652 Paustenbach, D.J. (2000). The Practice of Exposure Assessment: A State-of-the-Art Review. *J.*
653 *Toxicol. Environ. Health Part B* 3, 179–291.

654 Peijnenburg, W.J.G.M., and Jager, T. (2003). Monitoring approaches to assess bioaccessibility and
655 bioavailability of metals: Matrix issues. *Ecotoxicol. Environ. Saf.* 56, 63–77.

656 Pelfrêne, A., Waterlot, C., Mazzuca, M., Nisse, C., Cuny, D., Richard, A., Denys, S., Heyman, C.,
657 Roussel, H., Bidar, G., et al. (2012). Bioaccessibility of trace elements as affected by soil
658 parameters in smelter-contaminated agricultural soils: A statistical modeling approach. *Environ.*
659 *Pollut.* 160, 130–138.

660 Pokrovsky, O.S., and Schott, J. (2000). Kinetics and mechanism of forsterite dissolution at 25°C
661 and pH from 1 to 12. *Geochim. Cosmochim. Acta* 64, 3313–3325.

662 Pouchou, J. L. & Pichoir, F. (1988). Determination of mass absorption coefficients for soft X-rays
663 by use of the electron microprobe. In: Newbury, D.E. (ed.) *Microbeam Analysis*. San Francisco,
664 CA: San Francisco Press, pp. 319-324.

665 Quantin, C., Ettler, V., Garnier, J., and Šebek, O. (2008). Sources and extractibility of chromium
666 and nickel in soil profiles developed on Czech serpentinites. *Comptes Rendus Geosci.* 340, 872–
667 882.

668 Redler, C., Johnson, T.E., White, R.W., and Kunz, B.E. Phase equilibrium constraints on a deep
669 crustal metamorphic field gradient: metapelitic rocks from the Ivrea Zone (NW Italy). *J.*
670 *Metamorph. Geol.* 30, 235–254.

671 Reis, A.P., Patinha, C., Wragg, J., Dias, A.C., Cave, M., Sousa, A.J., Costa, C., Cachada, A., Silva,
672 E.F. da, Rocha, F., et al. (2014). Geochemistry, mineralogy, solid-phase fractionation and oral
673 bioaccessibility of lead in urban soils of Lisbon. *Environ. Geochem. Health* 36, 867–881.

674 Rossetti P., Dino G.A., Biglia G., Costa E. (2017). Characterization of secondary raw materials
675 from mine waste: a case study from the Campello Monti Ni±Cu±Co±PGE mining site (Western
676 Alps, Italy). *Sardinia 2017 / Sixteenth International Waste Management and Landfill Symposium /*
677 *2 - 6 October 2017. S. Margherita di Pula, Cagliari, Italy / © 2017 by CISA Publisher, Italy. ISSN*
678 *2282-0027. pp.13. (Proceedings).*

679 Ruby, M.V., Schoof, R., Brattin, W., Goldade, M., Post, G., Harnois, M., Mosby, D.E., Casteel,
680 S.W., Berti, W., Carpenter, M., et al. (1999). Advances in Evaluating the Oral Bioavailability of
681 Inorganics in Soil for Use in Human Health Risk Assessment. *Environ. Sci. Technol.* 33, 3697–
682 3705.

683 Teien, H.-C., Kroglund, F., Atland, A., Rosseland, B.O., and Salbu, B. (2006). Sodium silicate as
684 alternative to liming-reduced aluminium toxicity for Atlantic salmon (*Salmo salar* L.) in unstable
685 mixing zones. *Sci. Total Environ.* 358, 151–163.

686 U.S. EPA 3051 A, 2007. Washington, DC, Microwave assisted acid digestion of sediments,
687 sludges, soils, and oils.

688 U.S. EPA 6010 C, 2007. Washington, DC, Inductivelycoupled plasma-atomic emission
689 spectrometry.

690 Venturelli, G., Contini, S., Bonazzi, A., and Mangia, A. (2016). Weathering of ultramafic rocks and
691 element mobility at Mt. Prinzera, Northern Apennines, Italy. *Mineral. Mag.* 61, 765–778.

692 Wickham H (2007). Reshaping Data with the Reshape Package. *J Stat Softw*, 21(12), 1-20.

693 Wickham H (2009). *ggplot2: Elegant Graphics for Data Analysis*. useR. Springer-Verlag.

694 Wragg, J. (2005). A study of the relationship between Arsenic bioaccessibility and its solid phase
695 distribution in Wellingborough soils. PhD Thesis, University of Nottingham.

696 Yao, Q., Wang, X., Jian, H., Chen, H., and Yu, Z. (2015). Characterization of the Particle Size
697 Fraction associated with Heavy Metals in Suspended Sediments of the Yellow River. *Int. J.*
698 *Environ. Res. Public. Health* *12*, 6725–6744.

699 Yunmei, Y., Yongxuan, Z., Williams-Jones, A.E., Zhenmin, G., and Dexian, L. (2004). A kinetic
700 study of the oxidation of arsenopyrite in acidic solutions: implications for the environment. *Appl.*
701 *Geochem.* *19*, 435–444.

702